Likelihood-Based Adaptive Learning in Stochastic State-Based Models

Peter Vieting[1], Rodrigo C. de Lamare[2], Lukas Martin[3], Guido Dartmann[45] and Anke Schmeink[15]

***Abstract*—This paper presents an adaptive learning framework for estimating structural parameters in stochastic state-based models (SSMs). SSMs are a useful modeling tool in systems biology and medicine. While models in these disciplines are traditionally hand-crafted, an automated generation based on experimental data becomes a topic of research interest. In particular, our goal is to classify measured processes using the generated models. An innovative likelihood-based adaptive learning approach capable of learning the structural parameters, i.e., the arc weights of SSMs from data and exploiting the reliability of detected inputs is presented in this work. Its convergence behavior is analyzed and an expression for the error at steady state is derived. Simulations assess the performance of the proposed and existing algorithms for a gene regulatory network.**

***Index Terms*—Bioinformatics and genomics, statistical learning, adaptive signal processing**

I. Introduction

MODELLING of complex systems may be performed using manifold approaches. One method often used in molecular and systems biology are Petri nets (PNs) [1], [2]. They have the advantage of a precise mathematical description of a model that can be illustrated at the same time. Various forms of PNs have been reported and tools have been developd for them [3], [4], [5], [6], [7], [8], [9], [10], [11]. In biomedical applications, PNs are particularly popular because of their ability to model concurrency which is a characteristic of reactions in biochemical systems [2]. Furthermore, they can be considered as a white box approach as their quantities and structure are interpretable and understandable unlike classical machine learning concepts such as neural networks.

Machine learning techniques have the potential to improve medical research and practice in many ways [12]. One possible way of integrating machine learning into the medical sector is through clinical decision support systems [13], [14], [15]. To develop such tools, freely accessible databases such as the MIMIC-III database may be targeted. It contains vital signs, laboratory measurements, diagnostic codes and more for large numbers of intensive care patients [16]. With this kind of high dimensional data, methods to understand relationships and estimate unknown processes are essential. For instance, data may be used to classify a given measurement as pathological or healthy. Approaches on different abstraction levels allow both individual decision support based on reliable models of patient-adapted pathophysiological processes and the improvement of drug design with models of in vitro experiments. Prior work includes different metaheuristics applied for parameter estimation [17] and a data assimilation approach based on particle filtering to approximate Bayesian estimators [18]. Furthermore, efforts to solve the network reconstruction problem have been presented to find all possible PNs that fit the observed experimental data [19], [20], [21].

This work proposes adaptive learning techniques capable of identifying the topology of stochastic models from observed data. Unlike [22], a more general and self-contained stochastic system model is considered. We develop an adaptive learning algorithm that exploits the reliability of detected inputs. We also carry out a stochastic analysis of the proposed algorithm and evaluate its performance through simulations.

This paper is structured as follows: In Section II, we describe the system model. The proposed likelihood-based learning algorithm is presented in Section III. In Section IV, we study the adaptive techniques' convergence behavior and their performance is assessed by simulations in Section V before Section VI concludes the paper.

II. Stochastic State-Based Model

A bipartite graph with two types of nodes – places and transitions – constitutes the stochastic state-based model (SSM) used in this work. Similar to classical PNs [23], places contain tokens whereas the firing of transitions changes the network's marking and introduces dynamics into the model. Our SSM deploys an exponentially distributed random delay until an enabled transition fires, resembling stochastic Petri nets (SPNs) [23]. The transitions used here are single-servers and the model is assumed to be ergodic.

An exemplary SSM is given in Fig. 1. Places and transitions are denoted as p_i and τ_j and their total numbers as P and T, respectively. The marking of a place is $m(p_i)$ and the network's total marking is $\mathbf{m} = [m(p_1), \dots, m(p_P)]^\top$. The weight of the arc connecting p_i to τ_j is denoted as $[\mathbf{Pre}]_{i,j}$ while the arc from τ_j to p_i has weight $[\mathbf{Post}]_{i,j}$. The incidence matrix of the SSM is defined as $\mathbf{A} = \mathbf{Post} - \mathbf{Pre}$, $\mathbf{A} \in \mathbb{N}_0^{P \times T}$. We emphasize that this SSM is pure, i.e., no transition has any place as both input and output place. Consequently, the connection between p_i and τ_j is uniquely described by $[\mathbf{A}]_{i,j}$.

Problem Statement: The goal is to estimate the SSM's structure, i.e., the arc weights $\mathbf{A}$ describing its topology, based

[1]Research Area ISEK, RWTH Aachen University, Germany
[2]Center for Telecommunication Studies, Pontifical Catholic University of Rio de Janeiro, Brazil
[3]Department of Intensive Care and Intermediate Care, University Hospital RWTH Aachen, Germany
[4]Research Area Distributed Systems, Trier University of Applied Sciences, Environmental Campus, Trier, Germany, [5]Corresponding Author
This project was funded by the Federal Ministry of Education and Research (BMBF) grant 13GW0280C, 13GW0280D and 13GW0280E as part of the IMEDALytics project.

on noisy measurements of the markings $\tilde{\mathbf{m}}_k = \mathbf{m}_k + \boldsymbol{\eta}_k$ at discrete time instants k from the set of all sampling times $\mathbb{K}$ influenced by additive white Gaussian noise (AWGN) $\boldsymbol{\eta}_k \sim \mathcal{N}(\mathbf{0}, \boldsymbol{\Sigma})$, $\boldsymbol{\eta}_k \in \mathbb{R}^P$. The number of places is implicitly given by the dimension of $\tilde{\mathbf{m}}_k$. In this work, we will differentiate between a case where the number of transitions and their respective firing times are known during the learning process and a case where no such information is available.

Ultimately, the estimated structure parameters are intended for classification of the underlying processes. Therefore, an approximation of the non-negative integer entries of $\mathbf{A}$ and $\mathbf{m}$ is presented here. Furthermore, the conflict resolution and memory policies are not considered. A further examination of these properties to identify a valid PN is left for future work.

The achievable model complexity is limited by the sampling rate. This is illustrated in Fig. 2, where $m(p_1)$ is plotted over time. If only one transition fires between two consecutive samples (e.g., at t_1 and t_2), its effect on the marking may be estimated correctly. In case of multiple firings (e.g., at t_3 and t_4), the effects of multiple transitions are accumulated and their joint influence is learned. In this work, we assume the sampling rate is sufficiently high such that the true model complexity may be achieved.

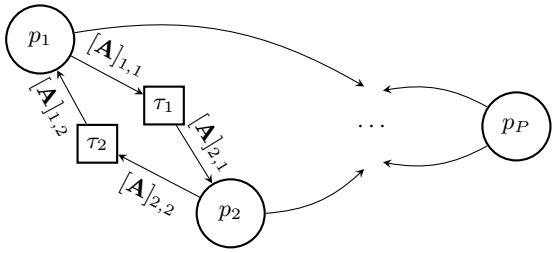

Fig. 1. Stochastic state-based model

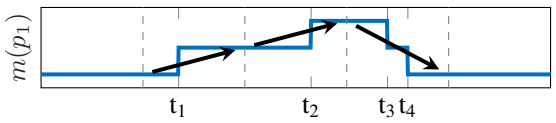

Fig. 2. Exemplary process realization. The sampling times are indicated by the dashed lines.

III. Proposed Adaptive Learning Approaches

In [22], adaptive learning approaches for hybrid systems are introduced. The foundation is a state space formulation and the state equation is given as $\mathbf{m}_{k+1} = \mathbf{m}_k + \mathbf{A} \cdot \mathbf{u}_k$ when considering only a stochastic system. The firing vector $\mathbf{u}_k$ states which transition fired at time instant k where element $[\mathbf{u}_k]_i \in \{0, 1\}$ represents τ_i. Based on the instantaneous mean squared error (MSE) as the objective function, an approach called gradient descent with full knowledge (GDFK) is derived and the resulting update equation reads as

$$\begin{aligned}\hat{\mathbf{A}}_{k+1} &= \hat{\mathbf{A}}_k - \mu' \cdot \nabla_{\hat{\mathbf{A}}_k} \widehat{\mathrm{MSE}}_{k+1} \\ &= \hat{\mathbf{A}}_k - \mu \cdot (\hat{\mathbf{m}}_{k+1} - \tilde{\mathbf{m}}_{k+1}) \cdot \mathbf{u}_k^\top,\end{aligned} \tag{1}$$

where μ denotes the step size. Here, $\mathbf{u}_k$ is assumed to be given $\forall\, k$. To overcome the need to know all firing instants, a maximum likelihood estimator (MLE) is proposed to estimate the firing vectors $\mathbf{u}_k$. New transitions are detected in a fashion resembling event-triggered control by monitoring a triggering condition. If this condition is met, a new transition is initialized. The approach is referred to as decision-aided adaptive gradient descent (DAAGD). These techniques are applicable to the proposed SSM by considering only the stochastic part of the network.

A. Likelihood-Based DAAGD (LB-DAAGD)

The DAAGD algorithm with its firing MLE from [22] always takes a hard decision on the most likely firing vector $\hat{\mathbf{u}}_k$. This is done by choosing the firing vector with the highest log-likelihood ratio (LLR)

$$\mathrm{LLR}(\mathbf{u}_k) = \log \frac{\Pr\left(\tilde{\mathbf{m}}_{k+1} | \tilde{\mathbf{m}}_k, \mathbf{u}_k\right)}{\Pr\left(\tilde{\mathbf{m}}_{k+1} | \tilde{\mathbf{m}}_k, \overline{F_k}\right)}, \tag{2}$$

where, based on the Gaussian noise, $\Pr\left(\tilde{\mathbf{m}}_{k+1} | \tilde{\mathbf{m}}_k, \mathbf{u}_k\right) = \frac{1}{(2\pi)^{P/2} \det(\boldsymbol{\Sigma}')^{1/2}} e^{-\frac{1}{2}\left(\Delta\tilde{\mathbf{m}}_k - \hat{\mathbf{A}}_k \cdot \mathbf{u}_k\right)^\top \cdot \boldsymbol{\Sigma}'^{-1} \cdot \left(\Delta\tilde{\mathbf{m}}_k - \hat{\mathbf{A}}_k \cdot \mathbf{u}_k\right)}$ with $\boldsymbol{\Sigma}' = 2\boldsymbol{\Sigma}$ and $\overline{F_k}$ is an indication that no transition fired, i.e., $\mathbf{u}_k = \mathbf{0}$. Please note that as (2) is normalized by the probability of no firing, it holds that $\mathrm{LLR}(\hat{\mathbf{u}}_k) \geq 0$.

The fact that these LLRs contain useful information about the reliability of the detection of firings inspires the idea of using them to improve the learning performance. Weighting the coefficient updates based on the reliability of the estimate $\hat{\mathbf{u}}_k$ by defining a dynamic convergence factor and therefore varying the step size allows us to incorporate this concept. In each time instant, the convergence factor consists of a constant factor μ_c and a weight depending on the LLR according to

$$\mu(k) = \mu_\mathrm{c} \cdot f\Big(\mathrm{LLR}\big(\hat{\mathbf{u}}(k)\big)\Big). \tag{3}$$

The LLR is mapped to the weighting interval via a function $f : \mathbb{R}_0 \to [0, 1]$. As a heuristic, we use $f(x) = 1 - e^{-2\alpha \cdot x}$. Thus, the LB-DAAGD identifies $\hat{\mathbf{u}}_k$ by finding the firing vector that maximizes the LLR expression in (2), predicts the next marking according to $\hat{\mathbf{m}}_{k+1} = \tilde{\mathbf{m}}_k + \hat{\mathbf{A}}_k \hat{\mathbf{u}}_k$ and updates the weights as stated in (1) using $\mu(k)$ from (3).

IV. Stochastic Analysis

This section studies the convergence behavior of the GDFK and LB-DAAGD algorithms. Similar goals are pursued in literature for other least mean squares (LMS)-type algorithms using the independence theory [24], [25], [26].

The error in the weight estimates at time instant k is defined as $\Delta\mathbf{A}_k = \hat{\mathbf{A}}_k - \mathbf{A}$. Thus, subtracting $\mathbf{A}$ from (1) while using $\mu_k = \mu(k)$ and $\hat{\mathbf{u}}_k$ yields

$$\begin{aligned}\Delta\mathbf{A}_{k+1} =& \Delta\mathbf{A}_k - \mu_k \cdot (\hat{\mathbf{m}}_{k+1} - \tilde{\mathbf{m}}_{k+1}) \cdot \hat{\mathbf{u}}_k^\top = \dots \\ =& \Delta\mathbf{A}_k - \mu_k \cdot \big(\Delta\mathbf{A}_k \cdot \mathbf{u}_k + \Delta\mathbf{A}_k \cdot \Delta\mathbf{u}_k \\ &+ \mathbf{A} \cdot \Delta\mathbf{u}_k - \boldsymbol{\eta}'_{k+1}\big) \cdot \hat{\mathbf{u}}_k^\top \\ =& \Delta\mathbf{A}_k \cdot \big(\mathbf{I} - \mu_k \cdot \mathbf{u}_k \cdot \hat{\mathbf{u}}_k^\top\big) \\ &+ \mu_k \cdot \boldsymbol{\eta}'_{k+1} \cdot \hat{\mathbf{u}}_k^\top - \mu_k \cdot \hat{\mathbf{A}}_k \cdot \Delta\mathbf{u}_k \cdot \hat{\mathbf{u}}_k^\top,\end{aligned} \tag{4}$$

where $\Delta\mathbf{u}_k = \hat{\mathbf{u}}_k - \mathbf{u}_k$ and $\boldsymbol{\eta}'_k = \boldsymbol{\eta}_k - \boldsymbol{\eta}_{k-1}$ with $\boldsymbol{\eta}'_k \sim \mathcal{N}(\mathbf{0}, \boldsymbol{\Sigma}')$ and $\boldsymbol{\Sigma}' = 2 \cdot \boldsymbol{\Sigma}$.

A. Convergence Behavior of GDFK

Proposition 1. *The GDFK's coefficients converge in the mean for SSMs with live transitions and the algorithm is stable provided that*

$$0 < \mu < 2. \tag{5}$$

Proof. The analysis of the GDFK algorithm is conducted by setting $\mu_k = \mu$ and $\Delta\mathbf{u}_k = 0$ in (4). Using the independence theory means assuming among others that the sequence of $\mathbf{u}_k$ is statistically independent and Gaussian-distributed as well as independent of the coefficient error [26], which does not hold in the present case. To proceed without making improper assumptions on $\mathbf{u}_k$, there are two key ideas:

1.) So far, (4) is considered for all $k \in \mathbb{K} = \{0, 1, 2, \ldots, K\}$. Since $\mathbf{u}_k = \mathbf{0}$ for many k, there is no change in the coefficient errors in these time instants. Therefore, (4) holds for a subset of time instants as well, namely $k' \in \mathbb{K}'$, where $\mathbb{K}'$ is a set containing only those time instants where a firing occurs, i.e., $||\mathbf{u}_{k'}|| \neq 0 \; \forall\, k'$. Using only $k' \in \mathbb{K}'$, the adaptive update equation (1) still holds and for all $k \notin \mathbb{K}'$, $\hat{\mathbf{A}}_k = \hat{\mathbf{A}}_{k^*}$ with $k^* = \max(k' \in \mathbb{K}', k' \leq k)$. Hence, it is sufficient to study $\Delta\mathbf{A}_{k'}, k' \in \mathbb{K}'$.

2.) Each column of $\mathbf{A}$ represents one SSM transition. Since we assume that only one discrete transition fires per time instant, at maximum one column of $\hat{\mathbf{A}}_k$ is updated at a time in (1). This allows separating the problem into single transitions and studying the convergence of the coefficients column-wise.

Consequently, we consider the τ^{th} column $\mathbf{a}$ of $\mathbf{A}$ representing transition τ. Let ${\mathbb{K}'}_\tau$ be a set containing only those time instants where τ fires, hence, $\left[\mathbf{u}_{k'}\right]_\tau = 1 \; \forall\, k' \in {\mathbb{K}'}_\tau$. Then, we adapt (4) and for all $k' \in {\mathbb{K}'}_\tau$ it holds that

$$\begin{aligned}\Delta\mathbf{a}_{k'+1} &= \Delta\mathbf{a}_{k'} - \mu \cdot (\hat{\mathbf{m}}_{k'+1} - \tilde{\mathbf{m}}_{k'+1}) \cdot \left[\mathbf{u}_{k'}^\top\right]_\tau = \ldots \\ &= \Delta\mathbf{a}_{k'} \left(1 - \mu \cdot \left[\mathbf{u}_{k'}\right]_\tau \left[\mathbf{u}_{k'}^\top\right]_\tau\right) + \mu \cdot \boldsymbol{\eta}'_{k'+1} \left[\mathbf{u}_{k'}^\top\right]_\tau \\ &= \Delta\mathbf{a}_{k'} \cdot (1-\mu) + \mu \cdot \boldsymbol{\eta}'_{k'+1},\end{aligned} \tag{6}$$

where the index $k'+1$ actually refers to the next k' in ${\mathbb{K}'}_\tau$, i.e., $\min(k^* \in {\mathbb{K}'}_\tau, k^* > k')$. For example, if ${\mathbb{K}'}_\tau = \{5, 7, 13, \ldots\}$, then as $k' = 7$ is considered in (6), $k'+1$ refers to 13.

Since the noise is assumed to have zero mean, the expectation of (6) reads as $\mathrm{E}\{\Delta\mathbf{a}_{k'+1}\} = \mathrm{E}\{\Delta\mathbf{a}_{k'}\} \cdot (1-\mu) = \mathrm{E}\{\Delta\mathbf{a}_0\}\,(1-\mu)^{k'+1}$. Then, the condition to guarantee convergence of the weights in the mean is that $(1-\mu)^{k'}$ vanishes for $k' \to \infty$, thus, $-1 < 1-\mu < 1$ which leads to (5).

Please note that considering the limit of $k' \to \infty$ requires that the set ${\mathbb{K}'}_\tau$ is infinite. In terms of the system model, that means transition τ is *live*, i.e., regardless of the evolution, transition τ will not become unfirable on a permanent basis [24]. Therefore, we have shown the convergence of the GDFK's coefficients in the mean for SSMs with live transitions.

To investigate the stability, the same ideas are helpful. As the mean value of $\Delta\mathbf{a}_{k'}^{\mathcal{S}}$ is zero for large k', the covariance matrix of the coefficient errors of transition τ is

$$\begin{aligned}\mathrm{cov}\left[\Delta\mathbf{a}_{k'+1}\right] &= \mathrm{E}\left\{\Delta\mathbf{a}_{k'+1} \cdot \left(\Delta\mathbf{a}_{k'+1}\right)^\top\right\} \\ &= \mathrm{E}\left\{(1-\mu)^2 \cdot \Delta\mathbf{a}_{k'} \left(\Delta\mathbf{a}_{k'}\right)^\top + \mu^2 \cdot \boldsymbol{\eta}'_{k'+1} \left(\boldsymbol{\eta}'_{k'+1}\right)^\top\right\} \\ &= (1-\mu)^2 \cdot \mathrm{cov}\left[\Delta\mathbf{a}_{k'}\right] + \mu^2 \cdot \boldsymbol{\Sigma}'.\end{aligned} \tag{7}$$

The GDFK algorithm is said to be stable if the diagonal elements of $\mathrm{cov}\left[\Delta\mathbf{a}_{k'}\right]$ converge. According to [25], a necessary and sufficient condition for this is that all the eigenvalues of the state matrix $(1-\mu)^2 \cdot \mathbf{I}$ in (7) lie inside the open unit disc. Therefore, $-1 < (1-\mu)^2 < 1$ which is equivalent to the condition for convergence in (5). □

Proposition 2. *The total MSE at firing instants in steady state (MSE_{ss}) consists of the minimum MSE (MSE_{min}) and the excess mean squared error (EMSE) at firing instants in steady state ($MSE_{\text{ex,ss}}$) and reads as*

$$MSE_{\text{ss}} = MSE_{\text{min}} + MSE_{\text{ex,ss}} = 2 \cdot tr\left[\boldsymbol{\Sigma}\right] + \frac{2\mu}{2-\mu} tr\left[\boldsymbol{\Sigma}\right]. \tag{8}$$

Proof. We now consider the full coefficient matrix again to obtain an expression for the EMSE. As $\mathbb{K}'$ contains all firing time instants of all SSM transitions now, it holds that $\mathbf{u}_{k'}^\top \mathbf{u}_{k'} = 1$. When studying the expectation of the coefficient error matrix' Frobenius norm for the firing instants $k' \in \mathbb{K}'$ and replacing the adaptation of (4) to GDFK $\Delta\mathbf{A}_{k'+1} = \Delta\mathbf{A}_{k'}\left(1 - \mu \cdot \mathbf{u}_{k'}\mathbf{u}_{k'}^\top\right) + \mu \cdot \boldsymbol{\eta}'_{k'+1}\mathbf{u}_{k'}^\top$, the cross terms of the noise cancel and it is possible to further manipulate the expression according to

$$\begin{aligned}\xi_{k'+1} &= \mathrm{E}\left\{\mathrm{tr}\left[\Delta\mathbf{A}_{k'+1}^\top \Delta\mathbf{A}_{k'+1}\right]\right\} \\ &= \mathrm{E}\Big\{\mathrm{tr}\Big[\left(1 - \mu \cdot \mathbf{u}_{k'}\mathbf{u}_{k'}^\top\right)^\top \Delta\mathbf{A}_{k'}^\top \cdot \Delta\mathbf{A}_{k'} \left(1 - \mu \cdot \mathbf{u}_{k'}\mathbf{u}_{k'}^\top\right)\Big]\Big\} \\ &\quad + \mu^2 \cdot \mathrm{E}\left\{\mathrm{tr}\left[\mathbf{u}_{k'}^\top \mathbf{u}_{k'} \left(\boldsymbol{\eta}'_{k'+1}\right)^\top \boldsymbol{\eta}'_{k'+1}\right]\right\} \\ &= \mathrm{E}\left\{\mathrm{tr}\left[\Delta\mathbf{A}_{k'}^\top \Delta\mathbf{A}_{k'}\right]\right\} - 2\mu \cdot \mathrm{E}\left\{\mathrm{tr}\left[\mathbf{u}_{k'}\mathbf{u}_{k'}^\top \Delta\mathbf{A}_{k'}^\top \Delta\mathbf{A}_{k'}\right]\right\} \\ &\quad + \mu^2 \cdot \mathrm{E}\left\{\mathrm{tr}\left[\mathbf{u}_{k'}\mathbf{u}_{k'}^\top \Delta\mathbf{A}_{k'}^\top \Delta\mathbf{A}_{k'} \mathbf{u}_{k'}\mathbf{u}_{k'}^\top\right]\right\} \\ &\quad + \mu^2 \cdot \mathrm{E}\left\{\mathrm{tr}\left[\mathbf{u}_{k'}^\top \mathbf{u}_{k'} \left(\boldsymbol{\eta}'_{k'+1}\right)^\top \boldsymbol{\eta}'_{k'+1}\right]\right\} \\ &= \mathrm{E}\left\{\mathrm{tr}\left[\Delta\mathbf{A}_{k'}^\top \Delta\mathbf{A}_{k'}\right]\right\} + \mu^2 \cdot \mathrm{E}\left\{\mathrm{tr}\left[\left(\boldsymbol{\eta}'_{k'+1}\right)^\top \boldsymbol{\eta}'_{k'+1}\right]\right\} \\ &\quad - 2\mu \cdot \mathrm{E}\left\{\mathrm{tr}\left[\mathbf{u}_{k'}^\top \Delta\mathbf{A}_{k'}^\top \Delta\mathbf{A}_{k'} \mathbf{u}_{k'}^{\mathcal{I}}\right]\right\} \\ &\quad + \mu^2 \cdot \mathrm{E}\left\{\mathrm{tr}\left[\mathbf{u}_{k'}^\top \Delta\mathbf{A}_{k'}^\top \Delta\mathbf{A}_{k'} \mathbf{u}_{k'}\right]\right\} \\ &= \xi_{k'} + \left(\mu^2 - 2\mu\right) \mathrm{MSE}_{\text{ex}}(k') + \mu^2 \cdot \mathrm{tr}\left[\boldsymbol{\Sigma}'\right].\end{aligned} \tag{9}$$

At steady state, $\xi_{k'} \to \xi_{k'+1}$. Therefore, we obtain an expression for the EMSE at firing instants at steady state

$$\mathrm{MSE}_{\text{ex,ss}} = \frac{2\mu}{2-\mu} \mathrm{tr}\left[\boldsymbol{\Sigma}\right]. \tag{10}$$

Adding the minimum MSE which is just the noise influence to the EMSE yields the total MSE at steady state as stated in (8). As only the firing instants are considered in (9), the EMSE expression in (10) is only valid for these time instants. In non-firing instants, there is no EMSE contribution and the MSE consists of the noise influence $\mathrm{MSE}_{\text{min}}$ only. □

B. Convergence Behavior of LB-DAAGD

When considering the LB-DAAGD, the algebraic manipulations allowing to move from (4) to (6) are not valid anymore, thus, the expressions cannot be reshaped in a way that all contributions of $\hat{\mathbf{u}}_k$ are ruled out. In order to proceed with the analysis, it is necessary to make assumptions. Note that they might not be strictly justified but still lead to reasonable results such as in [24]. Additionally, there cannot be a general guarantee that the LB-DAAGD algorithm detects the correct transitions due to the thresholding approach. It is bound to

fail if the noise power is too high ($\sigma^2 >> ||\mathbf{a}||$). Therefore, we assume that the signal-to-noise ratio (SNR) is sufficiently high to allow a correct transition detection. Then, it is possible that the learning scheme can compensate errors in the firing estimation and still approach the correct weights similar to the decision-directed method in adaptive equalization [26].

Based on (4), we assume independence of $\boldsymbol{\eta}'_{k+1}$ and $\hat{\mathbf{u}}_k$ as well as of $\Delta\mathbf{A}_k$ and $\mathbf{u}_k \cdot \hat{\mathbf{u}}_k^\top$, respectively. Additionally, $\mu_k \cdot \hat{\mathbf{A}}_k \cdot \Delta\mathbf{u}_k \cdot \hat{\mathbf{u}}_k^\top$ is considered as negligible compared to the other terms in (4) as indicated by the histograms in Fig. 3. Then, we obtain the simplified expectation

$$\begin{aligned}\mathrm{E}\left\{\Delta\mathbf{A}_{k'+1}\right\} &\approx \mathrm{E}\left\{\Delta\mathbf{A}_{k'}\right\} \cdot \left(\mathbf{I} - \mathrm{E}\left\{\mu_{k'} \cdot \mathbf{u}_{k'} \cdot \hat{\mathbf{u}}_{k'}^\top\right\}\right) \\ &= \mathrm{E}\left\{\Delta\mathbf{A}_0\right\} \cdot \left(\mathbf{I} - \mu_\mathrm{c} \cdot \mathbf{R}\right)^{k'+1},\end{aligned} \tag{11}$$

with $\mathbf{R} = \mathrm{E}\left\{f(\mathrm{LLR}(\hat{\mathbf{u}}_{k'})) \cdot \mathbf{u}_{k'} \cdot \hat{\mathbf{u}}_{k'}^\top\right\}$ and where again only the firing instants are considered.

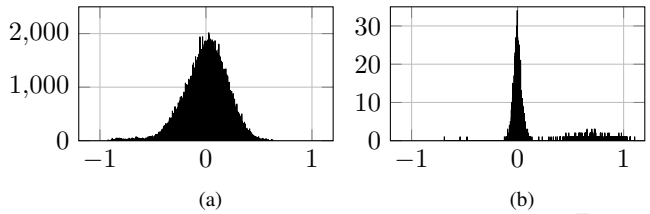

(a) (b)

Fig. 3. Histograms of the elements of (a) $\Delta\mathbf{A}_k \cdot \left(\mathbf{I} - \mu_k \cdot \mathbf{u}_k \cdot \hat{\mathbf{u}}_k^\top\right)$ and (b) $\mu_k \cdot \hat{\mathbf{A}}_k \cdot \Delta\mathbf{u}_k \cdot \hat{\mathbf{u}}_k^\top$ from (4) with the LB-DAAGD for $\mu_c = 0.3$, $\sigma^2 = 0.01$, $\mathrm{MSE_{th}} = 0.08$, $\alpha = 0.01$ and k sufficiently large such that all transitions are detected. The dominant peak at 0 in (b) with a value of more than 10^6 is not shown to allow seeing the other values. Time instants with $\mathbf{u}_k = \hat{\mathbf{u}}_k = \mathbf{0}$ are discarded. Note the different y-axis scales.

Now μ_c has to be chosen such that $\left(\mathbf{I} - \mu_\mathrm{c} \cdot \mathbf{R}\right)^{k'} \to 0$ for $k' \to \infty$ to guarantee the convergence of the coefficient error in the mean. This can be done by ensuring that the absolute values of all eigenvalues of $\mathbf{I} - \mu_\mathrm{c} \cdot \mathbf{R}$ lie between -1 and 1, hence, $0 < \mu_\mathrm{c} < \frac{2}{\max(|\lambda_i|)}$ with $\lambda_i \in \mathrm{spec}(\mathbf{R})$. For LB-DAAGD, the properties of $\hat{\mathbf{u}}_k$ and therefore the structure of $\mathbf{R}$ are not easily defined, however, in the special case of GDFK approach it simplifies to a diagonal matrix where the entry $[\mathbf{R}]_{ii} = p(F_i) \in [0, 1]$ corresponds to the firing probability of τ_i. Consequently, $\max(|\lambda_i|) = 1$ and the convergence condition coincides with (5).

V. Simulation Results

A (simplified) SSM model of a gene regulatory network of a circadian clock mechanism from [27] is used for validation of the learning schemes. A simple augmentation is used to allow converting the impure into a pure model [23]. A given realization is corrupted by noise and the approaches are applied. The coefficient MSE is computed by comparing $\hat{\mathbf{A}}_k$ to the true $\mathbf{A}$ according to $\mathrm{MSE}_k = \frac{1}{P \cdot T}||\hat{\mathbf{A}}_k - \mathbf{A}||_F^2$. For DAAGD and LB-DAAGD, each transition is compared to the transition that truly fired at the time instant of its detection. Undetected transitions in $\mathbf{A}$ are compared to $\mathbf{0}$. To allow a fair comparison, μ is set to 1 for each transition's first firing in GDFK as it is done in DAAGD. Additionally, a curve for the gradient descent with imperfect knowledge (GDIK) is included where the prior knowledge of firing instants is corrupted with a given bit error rate ($\mathrm{BER_u}$). Fig. 4 presents the results averaged over 50 realizations. The code is available online [28].

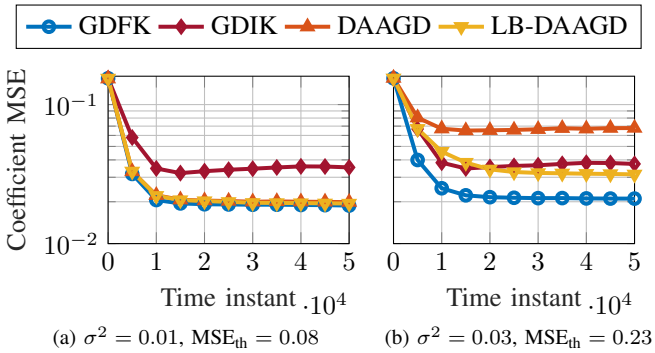

(a) $\sigma^2 = 0.01$, $\mathrm{MSE_{th}} = 0.08$ (b) $\sigma^2 = 0.03$, $\mathrm{MSE_{th}} = 0.23$

Fig. 4. Coefficient MSE for the different learning schemes with $\mu = 0.1$, $\alpha = 0.01$ and $\mathrm{BER_u} = 10^{-3}$.

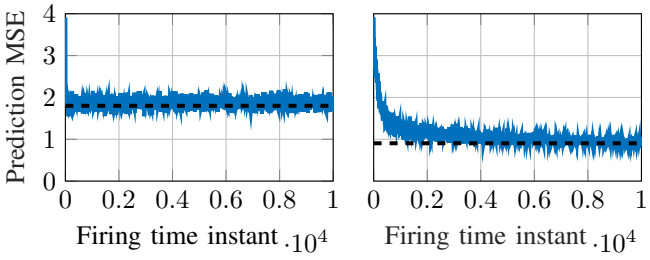

(a) (b)

Fig. 5. Prediction MSE during GDFK learning for (a) $\mu = 1$ and (b) $\mu = 0.01$ with $\sigma^2 = 0.03$. The blue curve shows simulations results while the dashed black curve depicts the theoretical value from (8).

It is clear that the coefficient MSE converges to a steady state for all techniques. Note that two transitions never fire which contributes an error of $1.5 \cdot 10^{-2}$ already. If they fired later, the MSE would change again as the statistics of these two transitions will be learned. For lower noise levels (Fig. 4a), the performance is similar for all methods and only GDIK falls short. As expected, for higher noise (Fig. 4b) GDFK with perfect knowledge about the firing instants performs best while the performance of DAAGD is considerably deteriorated. Using the reliability information in LB-DAAGD, DAAGD is clearly outperformed.

The theoretical expression of the MSE at steady state from (8) is compared to simulation results of GDFK in Fig. 5. Note that only values from firing time instants are considered here. The prediction MSE is calculated according to $\mathrm{MSE}_k = (\hat{\mathbf{m}}_k - \tilde{\mathbf{m}}_k)^\top \cdot (\hat{\mathbf{m}}_k - \tilde{\mathbf{m}}_k)$ and the results are averaged over 50 realizations. Fig. 5 shows that while the convergence speed is different, the simulation results approach the theoretically computed value for both choices of μ.

VI. Conclusion

In this paper, we have studied and developed adaptive learning techniques for the estimation of the relevant structure parameters of an SSM. Three approaches with different levels of prior knowledge and use of likelihood information are considered and their convergence behavior as well as their EMSE are analyzed. Simulations illustrate the algorithms' capability to learn parameters of a gene regulatory network and show the effectiveness of likelihood information that equips the proposed LB-DAAGD algorithm.

REFERENCES

[1] P. J. Goss and J. Peccoud, "Quantitative modeling of stochastic systems in molecular biology by using stochastic Petri nets," *Proceedings of the National Academy of Sciences*, vol. 95, no. 12, pp. 6750–6755, 1998.

[2] J. W. Pinney, D. R. Westhead, and G. A. McConkey, "Petri net representations in systems biology," 2003.

[3] W. M. Van der Aalst, "The application of Petri nets to workflow management," *Journal of circuits, systems, and computers*, vol. 8, no. 01, pp. 21–66, 1998.

[4] J. Billington and M. Diaz, *Application of Petri nets to communication networks: Advances in Petri nets*. Springer Science & Business Media, 1999, no. 1605.

[5] Z. Li and M. Zhou, "Elementary siphons of Petri nets and their application to deadlock prevention in flexible manufacturing systems," *IEEE Transactions on Systems, Man, and Cybernetics-Part A: Systems and Humans*, vol. 34, no. 1, pp. 38–51, 2004.

[6] A. Giua, M. Pilloni, and C. Seatzu, "Modelling and simulation of a bottling plant using hybrid Petri nets," *International journal of production research*, vol. 43, no. 7, pp. 1375–1395, 2005.

[7] S. M. Vahidipour and M. Esnaashari, "Priority assignment in queuing systems with unknown characteristics using learning automata and adaptive stochastic Petri nets," *Journal of computational science*, vol. 24, pp. 343–357, 2018.

[8] S. Vahidipour, M. Esnaashari, A. Rezvanian, and M. Meybodi, "GAPN-LA: A framework for solving graph problems using Petri nets and learning automata," *Engineering Applications of Artificial Intelligence*, vol. 77, pp. 255–267, 2019.

[9] S. M. Vahidipour, M. R. Meybodi, and M. Esnaashari, "Cellular adaptive Petri net based on learning automata and its application to the vertex coloring problem," *Discrete Event Dynamic Systems*, vol. 27, no. 4, pp. 609–640, 2017.

[10] Y. Xia, X. Luo, J. Li, and Q. Zhu, "A Petri-net-based approach to reliability determination of ontology-based service compositions," *IEEE Transactions on Systems, Man, and Cybernetics: Systems*, vol. 43, no. 5, pp. 1240–1247, 2013.

[11] Y. Xia, Y. Liu, J. Liu, and Q. Zhu, "Modeling and performance evaluation of BPEL processes: a stochastic-Petri-net-based approach," *IEEE Transactions on Systems, Man, and Cybernetics-Part A: Systems and Humans*, vol. 42, no. 2, pp. 503–510, 2012.

[12] Z. Obermeyer and E. J. Emanuel, "Predicting the futurebig data, machine learning, and clinical medicine," *The New England journal of medicine*, vol. 375, no. 13, p. 1216, 2016.

[13] A. Johnson, M. Ghassemi, S. Nemati, K. Niehaus, D. Clifton, and G. Clifford, "Machine learning and decision support in critical care," *Proceedings of the IEEE*, vol. 104, no. 2, pp. 444–466, 2016.

[14] T. Hemmerling, F. Cirillo, and S. Cyr, "Decision support systems in medicine - anesthesia, critical care and intensive care medicine," in *Decision Support Systems*. InTech, 2012.

[15] S. Pappada, T. Papadimos *et al.*, "Clinical decision support systems: From medical simulation to clinical practice," *International Journal of Academic Medicine*, vol. 3, no. 1, pp. 78–8, 2017.

[16] A. E. Johnson, T. J. Pollard, L. Shen, H. L. Li-wei, M. Feng, M. Ghassemi, B. Moody, P. Szolovits, L. A. Celi, and R. G. Mark, "MIMIC-III, a freely accessible critical care database," *Scientific data*, vol. 3, p. 160035, 2016.

[17] J. Sun, J. Garibaldi, and C. Hodgman, "Parameter estimation using metaheuristics in systems biology: a comprehensive review," *IEEE/ACM Transactions on Computational Biology and Bioinformatics (TCBB)*, vol. 9, no. 1, pp. 185–202, 2012.

[18] M. Nagasaki, R. Yamaguchi, R. Yoshida, S. Imoto, A. Doi, Y. Tamada, H. Matsuno, S. Miyano, and T. Higuchi, "Genomic data assimilation for estimating hybrid functional Petri net from time-course gene expression data," *Genome Informatics*, vol. 17, no. 1, pp. 46–61, 2006.

[19] M. Durzinsky, A. Wagler, and R. Weismantel, "An algorithmic framework for network reconstruction," *Theoretical Computer Science*, vol. 412, no. 26, pp. 2800–2815, 2011.

[20] W. Marwan, A. Wagler, and R. Weismantel, "A mathematical approach to solve the network reconstruction problem," *Mathematical Methods of Operations Research*, vol. 67, no. 1, pp. 117–132, 2008.

[21] M. Durzinsky, A. Wagler, and R. Weismantel, "A combinatorial approach to reconstruct Petri nets from experimental data," in *International Conference on Computational Methods in Systems Biology*. Springer, 2008, pp. 328–346.

[22] P. Vieting, R. C. de Lamare, L. Martin, G. Dartmann, and A. Schmeink, "An adaptive learning approach to parameter estimation for hybrid Petri nets in systems biology," in *IEEE Statistical Signal Processing Workshop (SSP)*, June 2018, pp. 543–547.

[23] R. David and H. Alla, *Discrete, Continuous, and Hybrid Petri Nets*. Springer, 2005.

[24] P. Diniz, *Adaptive Filtering: Algorithms and Practical Implementation*, 2nd ed. Norwell, MA, USA: Kluwer Academic Publishers, 2002.

[25] A. H. Sayed, *Adaptive filters*. Hoboken, NJ, USA: John Wiley & Sons, 2008.

[26] S. Haykin, *Adaptive filter theory*, 3rd ed. Upper Saddle River, NJ, USA: Prentice-Hall, Inc., 1996.

[27] M. Blätke, M. Heiner, and W. Marwan, "Biomodel engineering with Petri nets," in *Algebraic and Discrete Mathematical Methods for Modern Biology*. Elsevier, 2015, pp. 141–192.

[28] https://github.com/vieting/adaLearnSSM.